Geoderma 459 (2025) 117351

Contents lists available at ScienceDirect

Geoderma

journal homepage: www.elsevier.com/locate/geoderma

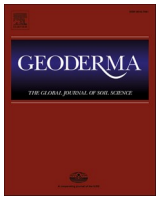

Elucidating the role of ferrihydrite and goethite in the aggregation and stability of small soil microaggregates: An experimental study on arable Luvisols under different management

Ni Tang [a,b,c,*], Nina Siebers [a,d], Stefan Dultz [e], Erwin Klumpp [a]

[a] Institute of Bio- and Geosciences, Agrosphere (IBG-3), Forschungszentrum Jülich GmbH, Wilhelm-Johnen-Straße, 52425 Jülich, Germany
[b] Institute for Environmental Research, Biology V, RWTH Aachen University, Worringerweg 1, 52074 Aachen, Germany
[c] Institute of Crop Science and Resource Conservation (INRES), Soil Science and Soil Ecology, University of Bonn, Nussallee 13, 53113 Bonn, Germany
[d] Ernst Ruska-Centre for Microscopy and Spectroscopy with Electrons (ER-C), Forschungszentrum Jülich GmbH, Wilhelm-Johnen-Straße, 52425 Jülich, Germany
[e] Institute of Earth System Sciences, Section Soil Science, Leibniz Universität Hannover, Herrenhäuser Straße 2, 30419 Hannover, Germany

ARTICLE INFO

Handling Editor: Dr Daniel Said-Pullicino

Keywords:
Soil microaggregation
Size distribution of aggregates
Surface charge
Aggregate stability
Iron oxides
Humic acid
Soil colloids

ABSTRACT

Iron oxides, exhibiting positive surface charge in most acidic to neutral soils, are key inorganic agents for microaggregate formation, especially via their electrostatic interactions with negatively charged surfaces on organic and inorganic soil compounds. Yet, little is known on the influence of Fe oxide properties, i.e., size, shape, and surface charge on the formation of soil microaggregates (SMA). Here the aggregation of < 20 μm small SMA fractions in the presence of either ferrihydrite or goethite as well as the stability of the resulting aggregates were examined. Water stable small SMA fractions were isolated from Ap-horizons of Stagnic Luvisols under different management (cropped and bare fallow), and both had an average diameter of ~ 6 μm. Ferrihydrite and goethite, respectively, were added as suspensions to small SMA fractions at 1 or 5 wt%. For comparison, humic acid (HA), a common fraction of soil organic matter, was added at 1 wt% in solution. Laser diffraction was applied to determine changes in the hydrodynamic diameter and the stability of the resulting aggregates. Addition of Fe oxides facilitated the formation of $3 - 10$ μm SMA, which probably resulted from their aggregation with < 3 μm particles in the small SMA fractions via electrostatic attraction. Moreover, changes in the particle size distribution also suggested that the addition of Fe oxides decreased the share of > 10 μm SMA, thereby increasing the abundance of $3 - 10$ μm small SMA as well. Here it is likely that attachment of Fe oxides on SMA caused a rearrangement of their structure leading to a closer packing of particles. A generally higher decrease in the abundance of > 10 μm SMA in the ferrihydrite addition implied a more efficient compacting effect of ferrihydrite than that of goethite. This was presumably due to the smaller size of ferrihydrite, which can decrease the steric hindrance and provide more contact points. Changes in the size distribution of small SMA fractions were more pronounced after the addition of 5.0 wt% Fe oxides compared to the 1.0 wt% ones. In contrast, adsorption of the added HA on SMA increased their negative surface charges and steric hindrance between them, thereby favoring their dispersion rather than aggregation. In the stability test, both ferrihydrite and goethite showed a less effective stabilizing effect on SMA at the bare fallow site than the cropped one. However, ferrihydrite generally revealed a better ability to stabilize < 1 μm colloids in the small SMA fraction than goethite for both sites. Here, our study provides new insights into the abilities of different Fe oxides to form and stabilize aggregates in soil microaggregation.

1. Introduction

Proper functioning of soil ecosystem services, i.e., supplying microbial habitat, element cycling, organic carbon preservation, and gas and water exchange, largely depends on the support of soil structure (Blanco-Canqui and Lal, 2004; Totsche et al., 2018). Soil structure has been proposed to be primarily shaped by the dynamic arrangement of aggregated solid compounds along with pore networks and non-

* Corresponding author at: Institute of Bio- and Geosciences, Agrosphere (IBG-3), Forschungszentrum Jülich GmbH, Wilhelm-Johnen-Straße, 52425 Jülich, Germany.
E-mail address: n.tang@fz-juelich.de (N. Tang).

https://doi.org/10.1016/j.geoderma.2025.117351
Received 26 November 2024; Received in revised form 13 May 2025; Accepted 15 May 2025
Available online 23 May 2025

aggregated soil particles (Dexter, 1988; Díaz-Zorita et al., 2002). Soil aggregation at different levels, i.e., micro- and macro- aggregation, with the participation of various soil compounds, such as soil organic matter (SOM), clay minerals, metal oxides, and carbonates, is thus important for the development of soil structure and the provision of soil functions (Garland et al., 2024). At the microaggregation level, electrostatic and short-range van-der-Waals interactions as well as outer and inner sphere complexes in the < 20 μm soil fraction are often involved (Kleber et al., 2015; Totsche et al., 2018). The formed soil microaggregates (SMA; <250 μm) may further contribute to macroaggregation as composite building units. However, growing evidence suggests that the type of binding agents, including organic gluing and inorganic cementing agents, as well as the binding mechanism, are likely to vary with the aggregation level. For instance, concerning the organic gluing agents, while soil macroaggregates (>250 μm) are often stabilized by roots or via physical enmeshment and compaction (Amézketa, 1999), soil organic matter (SOM) with microbial origin (e.g., polysaccharide and proteinaceous compounds) and/or at a higher decomposition level is more engaged in the formation of SMA (Lehmann et al., 2007). Nevertheless, less is known on the inorganic cementing agents at different aggregation levels, where iron oxides, hydroxides and oxyhydroxides (hereafter collectively termed "Fe oxides") are one of the ubiquitous inorganic aggregate forming materials in soils (Schwertmann and Taylor, 1989; Cornell and Schwertmann, 2003).

Fe oxides usually occur in the finest soil size fraction, i.e., nanoparticles (<100 nm) and/or colloids (<1 μm), and their ability to promote soil aggregation is often associated with their surface charge (Schwertmann and Taylor, 1989; Cornell and Schwertmann, 2003; Dultz et al., 2019). The relatively high point of zero charge (pzc) values of Fe oxides, ranging between pH 6.5–9 (Kosmulski, 2020), allow them to be positively charged in acidic to weak alkaline soils. Accordingly, interactions of Fe oxides via electrostatic forces with negatively charged OM or clay minerals (Tombácz et al., 2004; Dultz et al., 2019) lead to the formation of clay and silt sized organo-mineral or mineral–mineral associations, which can serve as composite building units of SMA. Moreover, Fe oxide coating on and/or bridging particles with negatively charged surfaces could also favor (micro)aggregation in soils (Guhra et al., 2019). The formed small (<20 μm) and large (20–250 μm) SMA can either exist in free form or get involved in the formation of macroaggregates, fostering a hierarchical aggregate organization in soils (Oades and Waters, 1991; Six et al., 2004). Along this size hierarchy, the stability of aggregates is commonly found to decrease with their increasing sizes, intimately associated with properties of their binding agents (Amézketa, 1999; Kaiser and Asefaw Berhe, 2014).

Aggregate stability, the ability of soil aggregates to maintain their structural integrity against external forces, is often assessed by changes in the size distribution or mean weight diameter of aggregates after being subjected to disruption forces in a wet form, i.e., rainfall simulation, wet sieving, sonication disruption, and chemical dispersion (Amézketa, 1999; Hu et al., 2023), but it can be evaluated in the dry form as well with i.e., mechanical crushing (Amelung et al., 2024; Felde et al., 2021). The linkage between the soil aggregate stability and Fe oxides has been evidenced in previous studies. For example, when Fe oxides act as binding agents, reductive dissolution of Fe oxides has been reported to destabilize aggregates in soils that undergo redox fluctuations (De-Campos et al., 2009; Henderson et al., 2012; Giannetta et al., 2022). In addition, a decreased stability and/or an increased disintegration of soil aggregates were commonly observed as Fe oxides were selectively removed using laboratory chemical extraction i.e., oxalate and dithionite-citrate-bicarbonate (DCB) extraction (i.e., Barberis et al., 1991; Jiang et al., 2014). Also, wet extraction suggests that the aggregate stability in many soils is often tightly correlated with the content of poorly crystalline Fe oxides rather than that of total Fe oxides (Duiker et al., 2003; Regelink et al., 2015). This is likely due to the fact that poorly crystalline Fe oxides, like ferrihydrite, tend to have a larger and more reactive surface area and smaller particle size than their crystalline counterparts, e.g., goethite and hematite (Cornell and Schwertmann, 2003), presumably being more reactive in soil particle binding processes. In addition, Fe oxides with a smaller size can more readily enter open connective pores of aggregates by infiltration of water. Moreover, they could be transported by water meniscus to the contact points of soil particles upon drying, which can fill and/or bridge the inter-particle space (Schwertmann and Taylor, 1989; Mitchell and Soga, 2005). In this case, Fe oxides serve as solid bridges and greatly increase the stability of resulting aggregates. Yet, poorly crystalline Fe oxides are generally more susceptible to the reductive dissolution than the crystalline ones, and the stability of aggregates bound by them is prone to decrease. Indeed, the influence of properties of Fe oxides, i.e., surface charges, size, and shape, particularly on the formation of SMA and their stability together with the relevant mechanisms behind remains less explored.

Apart from their intrinsic properties, the significance of Fe oxides for soil aggregation also depends on the nature of the soil matrix. The total and amorphous Fe contents in SMA < 250 μm reported in previous studies ranged between ~ 0.21 − 0.78 % and ~ 0.15 − 0.22 % for Luvisols (Fernández-Ugalde et al., 2013), 3.21 − 4.12 % and 0.16 − 0.22 % for Ultisols (Peng et al., 2015), 1.60 − 4.10 % and 0.37 − 0.42 % for Alfisols (Xue et al., 2019), 0.68 − 1.94 % and 0.14 − 0.43 % for Inceptisols, and 2.0 − 10.6 % and 0.04 − 0.30 % for Oxisols (Pinheiro-Dick and Schwertmann, 1996), respectively. Particularly in soils with relatively low organic carbon (OC) content, Fe oxides alone or together with other cementing agents (i.e., silica, carbonates, clay minerals, and Al oxides) were proposed as main binding agents for the formation of aggregates (Six et al., 2004). This is often the case for tropical soils, i.e., Oxisols. However, in temperate soils, Duiker et al. (2003), for instance, found that the contribution of especially poorly crystalline Fe oxides to stabilize macroaggregates equals or even exceeds that of OC in B horizons of Alfisols. For arable soils, agricultural managements like bare fallow can induce the depletion of OC and thereby causing deficiency of organic gluing agents. In some cases, the importance of other binding agents in soil aggregation thus rises. For instance, a transition of the main binding agent has been reported for arable Andisols under different managements (Wagai et al., 2018), where an increasing contribution of reactive metals and older C as binding agents to aggregate formation was observed in the soil under bare fallow, resulting in the prevalence of aggregates with middle density (2.0–2.5 g cm^{-3}). Conversely, with the input of composts, aggregates were dominantly bound by the fresh-OM rendering a relatively high abundance of aggregates with lower density in the soil without tillage. Concerning the investigated soils in this study, 15 years of bare fallow led to a decreased mass and stability of macroaggregates and moreover loss of large SMA (53–250 μm; Schweizer et al., 2024; Siebers et al., 2024), which could be attributed to a decrease of the gluing effect of OM potentially due to a change in the OM composition (Schweizer et al., 2024). Instead, the poorly crystalline Fe oxides were assumed to be more important in stabilizing occluded SMA with smaller sizes (20–53 μm) in comparison to large occluded SMA (53–250 μm), especially at the cropped site (Siebers et al., 2024). Yet, it remains unknown, (i) for the studied bare fallow site, if Fe oxides can act as binding agents in the aggregation of small SMA fraction (< 20 μm) and compensate for the deficiency of fresh organic gluing agents, leading to the development and stabilization of large size (micro)aggregates; (ii) to what extent the aggregation behavior and stability of the resulting aggregates varied with the type of Fe oxides.

In the current study, we thus investigated the potential impacts of the type (ferrihydrite and goethite) and amount (1 and 5 wt%) of added Fe oxides on the aggregation of free water stable small SMA fraction (< 20 μm), as well as on the stability of the resulting aggregates. The applied Fe oxide concentrations at 1 and 5 wt% correspond to Fe contents of 0.63 and 3.15 % for goethite and of 0.21 and 1.04 % for ferrihydrite, respectively, in the range of the Fe content in SMA mentioned above. The small SMA fractions were separated from Ap horizons of arable soils

(Stagnic Luvisol) under cropping and bare fallow management mentioned above. Suspensions containing either ferrihydrite or goethite were added to the small SMA fraction. Hereafter, the extent of aggregation and the stability of resulting aggregates were evaluated by laser diffraction. Furthermore, humic acid (HA), a chemical fraction of natural OM that has been reported to be closely associated with the aggregate formation and stability, was added to the small SMA fraction as well. Like many soil organic compounds, coatings of HA on soil particles often increase negative surface charges, in contrast to the effect of the Fe oxide addition. Therefore, the effects of HA addition were compared with those of Fe oxide addition in terms of repulsive and attractive electrostatic forces in soil microaggregation. We hypothesized that (i) the lack of the fresh OM input as gluing agent in the bare fallow site can be largely compensated by the added Fe oxides in the aggregation of small SMA promoting the formation of larger size aggregates; (ii) due to the small particle size and large specific surface area, ferrihydrite is more efficient in promoting the aggregation of small SMA by acting as a binding agent, and (iii) their incorporation in SMA leads to an increased aggregate stability.

2. Materials and methods

2.1. Soil sampling and size fractionation

The sampling site is located in Selhausen (50°52′08″ N, 6°26′59″ E) which is a part of the German Lower Rhine Embayment and has been under arable management for at least 100 years. Detailed information on agricultural management, site descriptions, and sampling campaigns can be found in Schweizer et al. (2024). In brief, this study investigated the small SMA fraction separated from samples of the Ap horizons of two paired fields under different management. Both fields are in close vicinity within 100 m with one filed under continuous crop management (maize, winter wheat, and sugar beet) for a century. Conversely, another field has maintained bare fallow since 2005 with a regular application of glyphosate-based herbicides. Besides the usage of herbicide, a mechanical tillage was practiced to the top 5 cm annually between 2005 and 2010 (Meyer et al., 2017). In November 2019, the Ap horizons (5 − 25 cm) of the cropped and bare fallow fields were sampled from the west downslope, where the content of fine soil < 2 mm is relatively high compared to its counterparts in the east upslope. Two square sampling slots with a surface area of 1 m^2 were selected for the cropped and bare fallow sites, respectively (Fig. S1). In total 5 replicates were taken from these two slots after removing the upper 0 − 5 cm of the Ap horizons with a distance of ~ 1 − 1.4 m between the sampling points. Three of them were analyzed in the current study. According to the IUSS Working Group (2006), the soils belong to Stagnic Luvisol with a silt loam texture, although Stagnic properties are relatively weak and could not be observed in the Ap horizons (Tang et al., 2024). After sampling, the field-moist soil samples were sealed in plastic bags and preserved in a cool chamber at 4 °C until analysis. The average clay contents in the fine soil < 2 mm are 26.3 and 28.3 % for the cropped and bare fallow sites, respectively. For the fine soil of Ap horizons from the cropped and bare fallow sites, the oxalate extractable Fe (Fe_{ox}) were 2.53 ± 0.04 and 2.37 ± 0.04 g kg^{-1}, respectively, while the dithionite-citrate-bicarbonate extractable Fe (Fe_{DCB}) were 6.33 ± 0.07 and 7.38 ± 0.05 g kg^{-1}, respectively (Siebers et al., 2024). Moreover, these values in the occluded small SMA (<20 μm) were 3.96 (Fe_{ox}) and 7.74 (Fe_{DCB}) g kg^{-1} for the cropped site and were 3.68 (Fe_{ox}) and 8.50 (Fe_{DCB}) g kg^{-1} for the bare fallow site, respectively (Siebers et al., 2024).

The detailed description of the wet-fractionation and isolation of the < 20 μm fraction was stated in our previous publications on these soil samples (Siebers et al., 2024; Tang et al., 2024). Briefly, the field-moist soils samples were wet-fractionated with an automatic sieve tower with mesh sizes of 2800, 250, 53, and 20 μm and lasted for 10 min (Krause et al., 2018). After wet-sieving, the solid phase of the < 20 μm fraction (hereafter "small SMA fraction") was recovered from 11 L of suspension by centrifugation at 5346 × g for 8 min (Heraeus MULTIFUGE 4KR, Thermo 146 Scientific, Massachusetts, USA). The recovered solid was washed using Millipore water by repeated centrifugation and decantation until the electrical conductivity was ~ 5 μS cm^{-1}. To analyze the < 450 nm and < 1 μm colloids in the < 20 μm soil fraction, aliquots of the suspension containing the < 20 μm fraction were centrifuged for 13 min and 3 min at 9800 × g (Avanti JXN-30, Beckman Coulter, California, USA), respectively. The zeta potential of < 1 μm colloids was determined by dynamic light scattering (DLS; Nano ZS, Malvern Instruments, Malvern, UK). Elemental concentrations of OC, Si, Al, Fe, Ca, and Mg in the subsize fractions of < 450 nm colloids were obtained using the asymmetric flow field-flow fractionation (AF4, Postnova Analytics, Landsberg, Germany) coupled to an organic carbon detector (OCD; DOC laboratory Dr. Huber, Germany) and an inductively coupled plasma mass spectrometer (ICP-MS; Agilent 7500, Agilent Technologies, Japan). The separation channel of the AF4 was equipped with a 500 μm spacer and a 1 kDa PES membrane, and the injection volume of samples was 0.5 μ L. During the measurement, a 25 μM NaCl solution was used as the carrier solution. Details of the applied AF4 separation condition as well as of the identifying cutoff of the size fractions are available in Tang et al. (2024).

2.2. Preparation of Fe oxides and humic acid

Goethite was synthesized by addition of a 10 M NaOH solution to a 0.5 M $FeCl_3$ solution under continuous stirring up to a final pH of 12 (Atkinson et al., 1968). The suspension was then kept at 55 °C for 120 h. After adjusting pH 6 by addition of 0.1 M HCl, goethite was washed with deionized water by centrifugation and decantation until the electrical conductivity was < 20 μS cm^{-1}. A 2-line-ferrihydrite was prepared according to Schwertmann and Cornell (2008). Here 1 M KOH was added to a 0.2 M $Fe(NO_3)_3{\cdot}9H_2O$ solution under continuous stirring to reach a final pH of 7.5. The formed ferrihydrite was washed with deionized water by centrifugation and decantation. The average hydrodynamic diameters of the Fe oxides, measured by dynamic light scattering (Nano ZS, Malvern Instruments, Malvern, UK), were 203 and 553 nm for ferrihydrite and goethite, respectively. The isoelectric point (IEP) of goethite and ferrihydrite was determined from the zeta potentials at different pH values (Fig. S2) (Kosmulski, 2020). For zeta-potential measurement (Nano ZS, Malvern Instruments, Malvern, UK), 100 mg L^{-1} of ferrihydrite and goethite was suspended in 10 mM NaCl solution, and the pH of suspensions was adjusted by the addition of HCl or NaOH in the range of 4 − 10. The Fe oxide suspensions were then shaken for 20 h at 115 rpm under room temperature. Prior to the zeta potential measurement, the pH values of the suspensions were checked. The morphological information on ferrihydrite and goethite obtained by a scanning electron microscope (SEM; JEOL 7400F Oxford Instruments Inca, Tubney Woods, Abingdon, Oxon OX13 5QX, UK.) is shown in Fig. S3. Other detailed information on the characteristics of the ferrihydrite and goethite used is given in Gypser et al. (2018) and Dultz et al. (2019).

As a comparison for the Fe oxide treatments, a reference humic acid material (HA; Nordic Lake, 1R105H) purchased from the International Humic Substance Society (IHSS; Denver, Colorado, USA) was included. Information on properties of this HA reference was retrieved from the website of IHSS (https://humic-substances.org) and is shown in Table S1. The preparation of HA solution followed the procedure of Yang et al. (2019) and Gui et al. (2021). After adding 64 mg HA powder into 128 mL of 10 mM NaCl solution, a few drops of 0.1 M NaOH were added to assist the dissolution of HA. The HA solution was then shaken for 24 h at room temperature on a horizontal shaker. Hereafter, the pH value was adjusted to ~ 6.8 by using 0.1 M HCl and finally filtered with a 1 μm membrane filter to remove the undissolved materials. The "HA solution" was then measured with the AF4-OCD and the result suggested that HA was dominantly present in the size range 0.7–55 nm while a small portion of HA colloids were between 55–270 nm (Fig. S4). Furthermore,

the total organic carbon (dissolved and colloidal form) concentration in the HA solution was 480 mg L^{-1} which was determined by AF4-OCD measurements with the crossflow rate at 0 mL min^{-1} (without the size fractionation) for 20 min.

2.3. Aggregation experiment

The aggregation experiment was performed using the wet-state < 20 μm small SMA fraction with either goethite or ferrihydrite in 10 mM NaCl suspensions. The mass ratios of Fe oxides in the Fe oxides-small SMA mixture were kept at 1 and 5 wt%, and the solid (g) to liquid (mL) ratio was maintained at 1:20. Before mixing with the small SMA fraction, the Fe oxide suspensions were dispersed in an ultrasonic bath. In comparison, the small SMA fraction was also added into HA solution without addition of Fe oxides (hereafter, referred to "HA treatment"). Furthermore, suspensions containing only the small SMA fraction in 10 mM NaCl without either Fe oxide or humic acid additions were included as controls. The pH values of suspensions were in the range of 6.8 − 7.2, and each treatment was conducted in triplicates. It is noteworthy that in the current experimental pH range the added Fe oxides had a tendency of homoaggregation and could be partially present as Fe oxide aggregates, potentially behaving differently from the system with monodispersed Fe oxides. The suspensions were then shaken on a horizontal shaker under room temperature at 75 rpm for 20 h. The pH values of selected samples were measured after the aggregation experiment. For the ferrihydrite addition treatments, the pH values were on average 6.7 slightly lower than the initial ones, while the pH values for the control, goethite, and HA addition treatments were on average 6.8, 6.9, and 6.9, respectively, comparable to the initial ones. Afterwards, for all the treatments, the particle size distribution was directly determined in suspension by laser diffraction (LA-950, Horiba, Kyōto, Japan). Moreover, subsamples of < 1 μm and < 450 nm soil colloids in the control and HA treatments were isolated by centrifugation. The zeta potential and elemental concentrations were determined for the isolated < 1 μm and < 450 nm soil colloids, respectively. The remaining part of the suspensions were shock frozen in liquid nitrogen and freeze-dried for electron microscopy.

2.4. Particle size distribution and stability assessment

The volume-based particle size distribution was measured using laser diffraction before and after the aggregation experiment in the wet form. The measurement was carried out under continuous stirring in a flow-through cell where light in two wavelengths (650 and 405 nm) was applied. The volume-based size distribution was calculated according to the Mie-theory, in which all the measured particles are assumed to be spherical, isotropic, and optically homogeneous (Bieganowski et al., 2018).

In addition, laser diffraction was also employed to assess the stability of aggregates resulting from the aggregation experiment with Fe oxides, adapting the methods of Mason et al. (2011) and Kasmerchak et al. (2019). Since aggregates were subjected to a constant and continuous shearing force when being stirred and circulated (Kasmerchak et al., 2019), a stability test could be achieved by monitoring changes in the size distribution and median size (D50) of particles over time via repeated measurements. D50 represents the size where the diameter of half of the detected particles is above this value and the diameter of the rest half is below this value. This procedure lasted for 40 min, with each measurement taking about 40 s. In the first 10 min, 10 size distribution measurements were conducted, whereas within the next 30 min measurements were performed every 3 min.

2.5. Scanning electron microscopy (SEM)

Since the freeze-drying was found to produce the least aggregation and thus largely preserve the segregated status in the wet form of particles compared to the air-drying (Siebers et al., 2018), the SMA were shock frozen in liquid nitrogen and freeze-dried prior to the SEM measurement. The freeze-dried SMA were analyzed using SEM. The JEOL 7400F is a SEM equipped with a cold field emission gun and primarily to be used for analysis where ultra-high resolution is required. Dried samples were prepared for SEM by spreading them onto a double-sided carbon tape and mounting onto a sample holder. Samples were subjected to a sputter coating, i.e., deposition by sputtering of an approximately 10 nm-thick Au-film onto the sample, in order to minimize charging effects. Images were recorded either at 10 or 20 keV.

2.6. Statistics

Statistical analysis was conducted in Origin (OriginPro 2022, Originlab, Massachusetts, USA). The normality of data distribution and homogeneity of variances were tested with the Shapiro-Wilk and Brown–Forsythe tests, respectively. The size distributions of small SMA in the Fe oxide and HA addition treatments were compared with the control treatments via the percentage of their overlapping area (Krause et al., 2020). The differences among treatments on small SMA from field replicates of soil samples was assessed statistically with a two-tailed *t*-test at a significant level of $\alpha = 0.05$. Three variables including the soil management (cropped vs bare fallow), the type of Fe oxide (goethite vs ferrihydrite), and the addition dosage (1 wt%, and 5 wt%), as well as potential interactions among these variables were considered when evaluating differences in the percentage of small SMA in different size ranges among treatments after the aggregation experiment. If the normality of data distribution and homogeneity of variances were valid, three-way ANOVA was performed with a Bonferroni post hoc test at a significant level of $\alpha = 0.05$. When the normality of data distribution and/or homogeneity of variances were violated, nonparametric tests including Kruskal-Wallis ANOVA ($P < 0.05$) and Wilcoxon rank-sum test ($\alpha = 0.05$) were conducted for comparison differences among different treatments within a given soil and differences between different soils within a given treatment, respectively. Moreover, one-way ANOVA was carried out to evaluate the differences at the end of the stability test in terms of the changes in the d50 and percentages of small SMA with different sizes among treatments within a give soil with a least significant difference post hoc test at a significant level of $\alpha = 0.05$.

3. Results

3.1. Changes of size distribution in the small SMA fractions among treatments

In the control, for both the cropped and bare fallow soils, the volume-based size distribution of the small SMA fraction was comparable, exhibiting a bimodal pattern for the diameter with peak maxima at 0.3 and 6.8 μm, respectively (Fig. 1). Particles with diameters between 1 − 20 μm accounted for ~ 93 vol% of the detected particles, while 6 vol% and < 1 vol% of particles were present in the size ranges of 0.1 − 1 and 20 − 40 μm, respectively. The D_{50} values of the small SMA fraction from the cropped and bare fallow Ap horizons were 6.2 ± 0.3 and 6.3 ± 0.1 μm, respectively.

The addition of either goethite or ferrihydrite generally changed the size distribution of the small SMA fraction compared to the control, although these changes varied with the dosage and type of Fe oxides as well as the soil sample (Fig. 1). For the small SMA fraction from Ap horizons of both the cropped and bare fallow sites, significant changes were observed for all 5 wt% Fe oxide additions, where the abundance of 3 − 10 μm particles prominently increased in concomitant with a decrease of the share of < 3 and > 10 μm particles (Table S2 and S3). Consequently, in most of these treatments (Fig. 1a–c), the size distribution of small SMA fractions transformed into a unimodal pattern between 1.3 − 26.0 μm, being significantly different from that of the control treatments. Unlike the 5 wt% addition treatments, with 1 wt% Fe

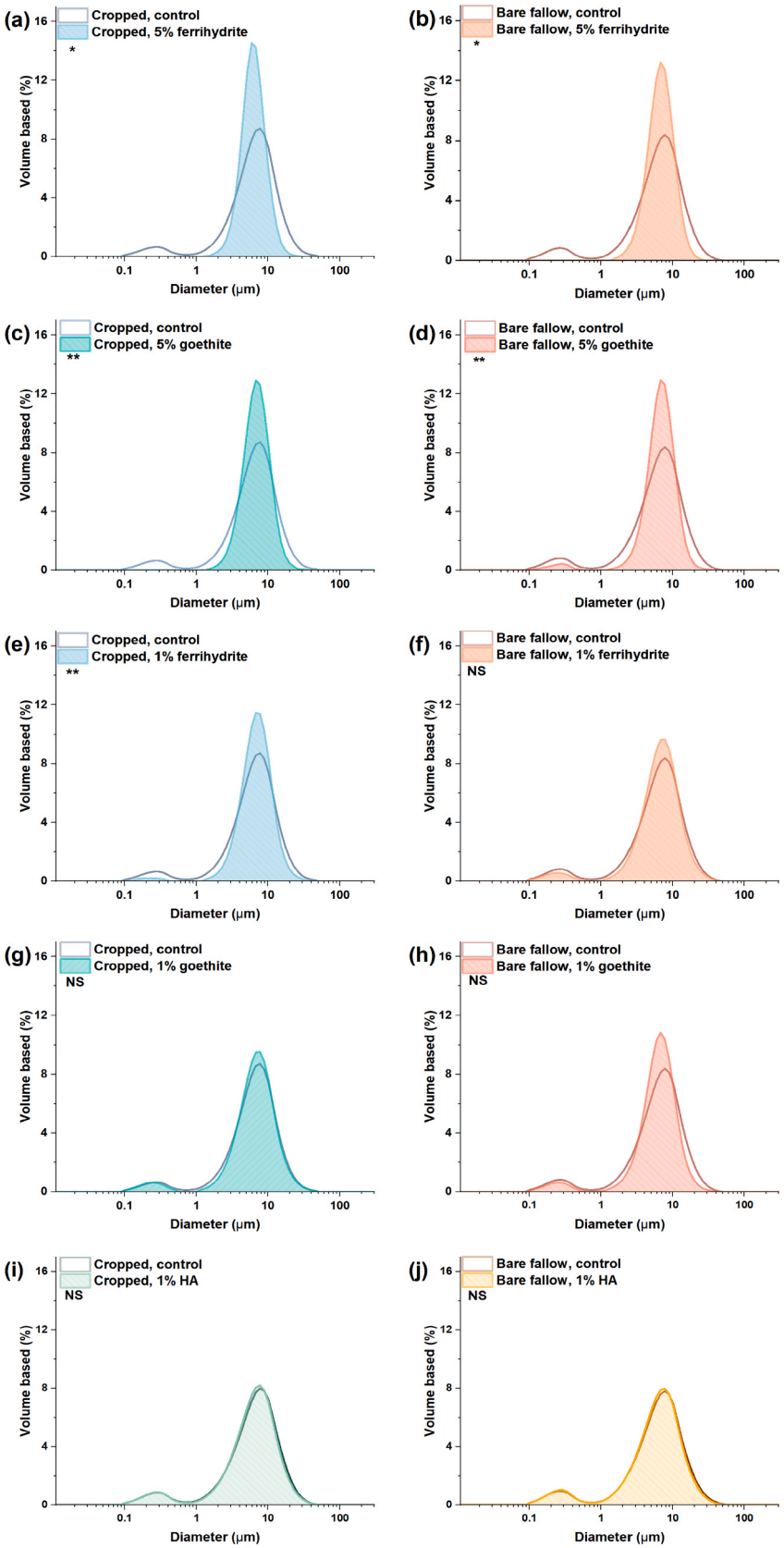

Fig. 1. Volume based size distributions of the small SMA fraction < 20 μm in the Fe oxide and humic acid (HA) addition treatments, and controls (pristine suspensions of the small SMA fraction). In the Fe oxide addition treatments, different dosages of ferrihydrite at 5 (a, b) and 1 wt% (e, f) and goethite at 5 (c, d) and 1 wt% (g, h) were added to small SMA fractions separated from Ap horizons from the cropped and bare fallow sites, respectively. In the HA treatment 1 wt% humic acid was added to the small SMA fraction (i, j). Significant differences in the size distribution between Fe oxide and HA addition treatments and controls are indicated in asterisks with $p \leq 0.05$, * and $p \leq 0.01$, **, while non-significant difference ($P > 0.05$) is marked with NS.

oxide addition (Fig. 1e–h) the particles size distribution remarkably changed only when the small SMA fraction from the cropped soil was treated with ferrihydrite (Fig. 1e). In contrast to the Fe oxide treatments, the HA treatments for both the cropped and bare fallow soils showed no significant changes in the size distribution of small SMA fractions (Fig. 1i and j).

Based on the AF4 measurement of the < 450 nm colloids in the small SMA fraction for the control and HA treatment, three subsize fractions, 0.7 – 55, 55 – 270, and 270 – 450 nm, were separated (Fig. 2). In the control, the 0.7 – 55 nm fraction mainly comprised OC, Ca, Mg, and Si, while the 55 – 270 nm and 270 – 450 nm fractions exhibited comparable composition with high abundances of Si, Al, OC, and Fe (Fig. 2a). Moreover, the 55 – 270 nm fraction comprised 85 – 90 % of the measured 0.7 – 450 nm colloidal Si, Al, OC, and Fe. Compared to the control treatments, the addition of HA (<270 nm colloids) not only notably increased the OC content in the 0.7 – 55 nm and 55 – 270 nm fractions, but also the Al, Si, and Fe contents in the < 450 nm colloids, especially those in the 55 – 270 nm fractions (Fig. 2b). Moreover, the addition of HA resulted in a decrease in zeta potential values of the < 1 μm colloids in small SMA fractions from −26.6 ± 1.0 and −25.9 ± 0.7 mV to −31.9 ± 0.9 and –32.1 ± 1.0 mV for the cropped and bare fallow soils, respectively.

3.2. Effect of the Fe oxide addition on micromorphology of SMA

As revealed by SEM, the added ferrihydrite and their clusters exhibited a nearly spherical shape while the typical needle shape was observed for the added goethite (Fig. S3). Regarding the morphological characteristics of freeze-dried SMA (Fig. 3 and S5), large aggregates with the size up to hundreds of micrometers occurred in all the treatments (Fig. S5), exceeding the upper size limits (~ 40 μm) of their counterparts measured by laser diffraction in suspension (Fig. 1). Drying is generally known to promote the reaggregation of soil particles and aggregates in the wet form (Siebers et al., 2018). In the controls, most of the aggregates were relatively small and loosely connected to each other (Fig. S5a and S5b). Higher magnification revealed (Fig. 3) micro- and submicron-scaled structural features of aggregates, indicating that most of the colloidal and clay-sized particles have platelet-shaped appearance. These particles in the control treatment stacked and/or assembled in an edge-edge or face-face form, leading to a relatively loose and open structure (Fig. 3a and d). In contrast, with the addition of 5 % Fe oxide, large aggregates with a compact structure were observed, especially for the ferrihydrite addition (Fig. S5c and S5d), in which individual small aggregates barely occurred. Attachment of Fe oxides to colloidal and clay-sized platelets (Fig. 3b–c and e–f), as well as the coating on larger primary particles (i.e., Fig. 3e) were observed in the 5 % Fe oxide addition treatments. Consequently, denser structures formed in these treatments as soil particles were bridged and/or wrapped by Fe oxides.

3.3. Stability of SMA

In the stability test, where < 20 μm SMA were exposed to a constant mechanical force deriving from stirring, a decrease in D50 of SMA was observed for all treatments (Fig. 4a and b). This decrease in diameter was accompanied with an increased abundance of the 1 – 7 μm fraction (Fig. 4c and d; Table S4) and < 1 μm colloids (Fig. 4e and f; Table S4) to different extents. For SMA from the cropped soil, the D50 in most treatments rapidly decreased in the first 10 min, except for the 5 wt%

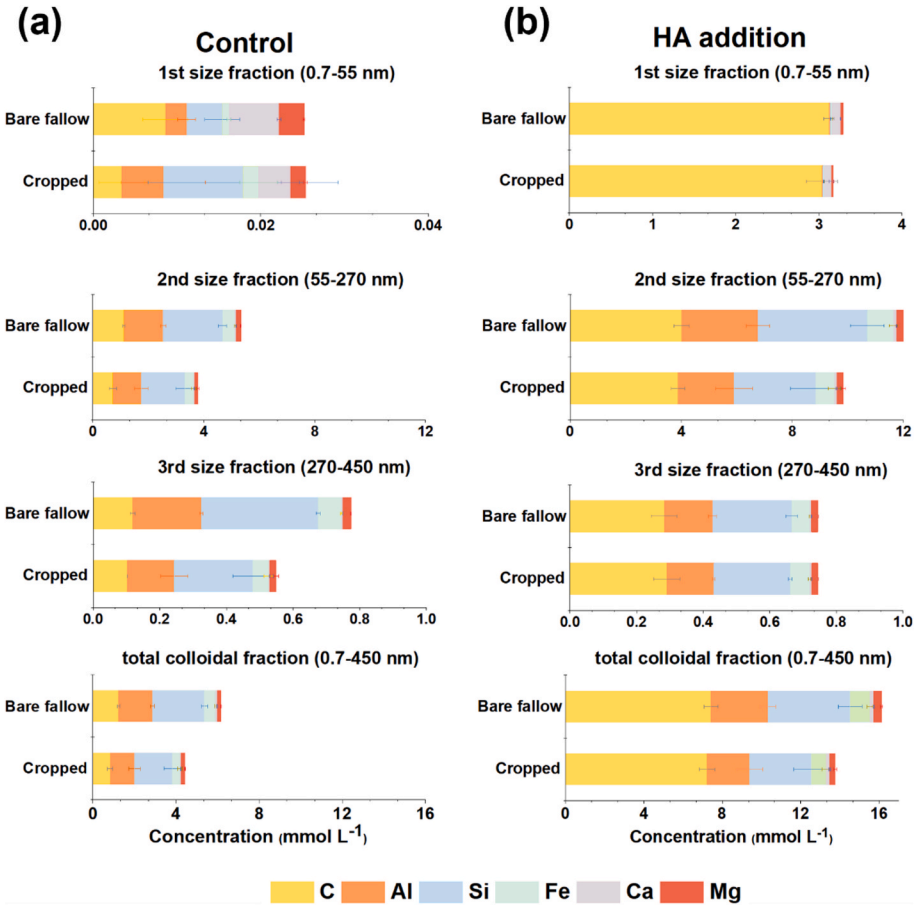

Fig. 2. Elemental concentrations in size fractions of the < 450 nm colloids in small SMA fractions < 20 μm from Ap horizons of the cropped and bare fallow site in the control (a; pristine suspensions of the small SMA fraction) and humic acid (HA) addition (b).

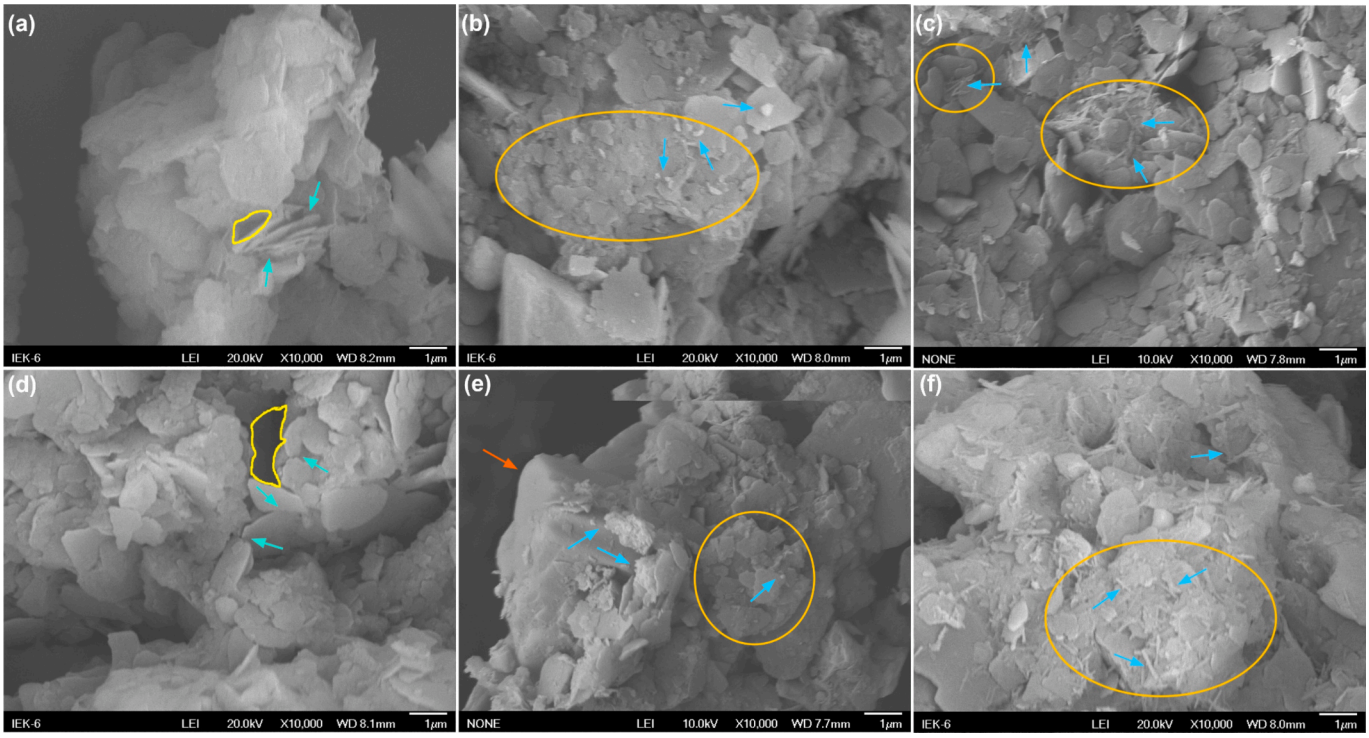

Fig. 3. Scanning electron microscopy (SEM) images of the small SMA fraction < 20 μm separated from the Ap-horizons of the cropped (a, b, and c) and bare fallow (d, e, and f) sites in the control (a and d), 5 wt% ferrihydrite (b and e), and 5 wt% goethite (c and f) additions. Scale bars are 1 μm. In control treatments, green arrows indicated loose structures that derived from face to face (a) and edge to edge (d) stacks of platy colloids, and yellow polygons pointed to open pores on SMA. In ferrihydrite addition treatments, blue and red arrows indicated ferrihydrite (particles and clusters; b and e) and primary particles (e), respectively; a compacted structure (b) and clay-sized aggregate (e) formed in the presence of ferrihydrite were highlighted by orange circles. Within which, attachment of ferrihydrite on colloids with platy shape could be also observed. In goethite addition treatments, goethite needles were shown by blue arrows (c and f), while clay-sized aggregates and /or dense structures of goethite and platy colloids were pointed by orange circles. (For interpretation of the references to colour in this figure legend, the reader is referred to the web version of this article.)

goethite addition treatment. This treatment also showed the least decline in the D50 over the 40 min measurement, while the decrease in D50 among other treatments was comparable (Fig. 4a). A similar trend was also found for the abundance of the 1 − 7 μm particles, with the 5 wt % goethite addition treatment showing a least increase in these particles (Fig. 4c), while their shares were increased by 11.5 − 13.4 vol% in the rest of treatments during the course of the stability test. However, the greatest release of < 1 μm colloids was found for the 5 wt% goethite addition treatment, whereas no release of < 1 μm colloids was observed in the 5 wt% ferrihydrite addition treatment (Fig. 4e; Table S4). The amount of released colloids < 1 μm in the 1 wt% Fe oxide addition treatments was similar to that in the controls. In contrast to the cropped soil, the bare fallow soil treated with 5 wt% of goethite and ferrihydrite, respectively, showed the rapidest decrease in the D50 of aggregates within the first 10 min. The largest decline in D50 was observed for the 5 wt% ferrihydrite treatment over the course of the stability test (Fig. 4b). This is corresponding to its largest increase in the percentage of the 1 − 7 μm particles among the different treatments (Fig. 4d; Table S4). The release of colloids was already observed in the 5 wt% goethite and ferrihydrite treatments within the first 10 min, and the former one possessed the largest release of colloids during the whole stability test (Fig. 4f; Table S4). The release of colloids in other treatments was at a comparable level.

4. Discussion

4.1. Small SMA fraction

For the studied Ap horizons, the effect of the agricultural management (cropped vs. bare fallow) on the OC content was reported to be more pronounced in the < 20 and 20 − 53 μm SMA (<2.5 g cm^{-3}; without the heavy fraction ≥ 2.5 g cm^{-3}, which can contain primary particles and mineral–mineral associations) than in the fine soil < 2 mm, as a trend toward lower OC contents was found in SMA < 2.5 g cm^{-3} from the bare fallow site (Siebers et al., 2024). After removal of the heavy fraction ≥ 2.5 g cm^{-3} using the density fractionation (Virto et al., 2008), the OC content in the free small SMA < 2.5 g cm^{-3} from the bare fallow site was 14.6 mg g^{-1} on average and significantly lower than that from the cropped site with 22.8 mg g^{-1} on average (Tang et al., 2024). However, the OC content in the small SMA fraction < 20 μm was found to be comparable for the cropped and bare fallow sites (on average 12.6 and 11.4 mg g^{-1}, respectively; Schweizer et al., 2024) in the presence of the heavy fraction ≥ 2.5 g cm^{-3}, which have a “diluting” effect on the OC concentration in the small SMA fraction from the both sites. In the current study, we did not remove the heavy fraction from the small SMA fraction, since the occlusion of particles ≥ 2.5 g cm^{-3}, like quartz, within SMA as their building units has been reported for other arable Luvisols (Schweizer et al., 2019; Felde et al., 2021). They were assumed to interact/aggregate with the added Fe oxides and/or HA, hereby contributing to the formation of SMA. Moreover, the presence of the heavy fraction did not change the size distribution pattern of the small SMA fraction for both the cropped and bare fallow sites, as the bimodal distribution peaking at 0.3 and 6.7 μm was also observed for small SMA < 2.5 g cm^{-3} from the same soils in our recent study (Tang et al., 2024).

Regarding the colloids (<1 μm) in the small SMA fraction, their negative zeta potentials (−26.6 ± 1.0 mV, cropped; −25.9 ± 0.7 mV, bare fallow) at circumneutral pH were in line with the previous findings of water dispersible colloids on the same site (Jiang et al., 2014), suggesting that positively charged surfaces appear to have a minor impact on the bulk surface charge of colloids in the small SMA fraction.

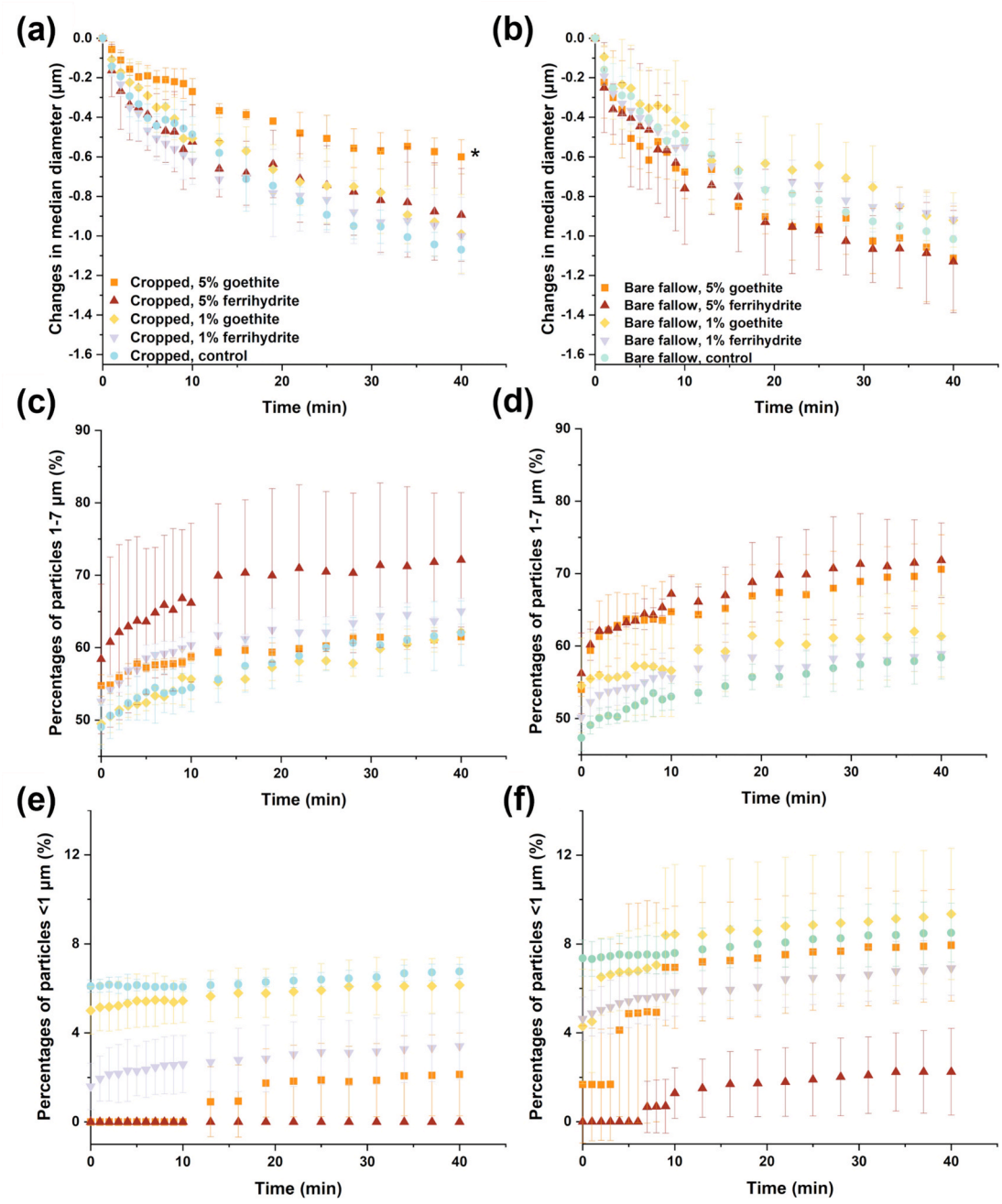

Fig. 4. Changes in the median diameter (D50; a and b) of small SMA < 20 μm and percentages of the 1 – 7 μm particles (c and d) and colloids (< 1 μm, e and f) in the stability test for the Fe oxide addition and control (pristine suspensions of the small SMA fraction). In the Fe oxide addition treatments, either goethite or ferrihydrite at dosages of 5 and 1 wt% was added to small SMA fractions < 20 μm from the Ap horizons of the cropped and bare fallow sites, respectively. Significant differences in changes in median diameter (D_{50}) among treatments within a given soil sample are indicated in asterisks with $p \leq 0.05$.

Moreover, as shown in the controls (Fig. 2a), the elemental composition of three subsize fractions (0.7 – 55 nm, 55 – 270 nm, and 270 – 450 nm) in the 0.7 – 450 nm soil colloids of the small SMA fractions were comparable to those in the small SMA < 2.5 g cm^{-3} after density fractionation (without primary particles > 2.5 g cm^{-3}) from the same soils (Tang et al., 2024), implying that the presence of primary particles scarcely affected the size distribution of the 0.7 – 450 nm colloidal fraction. However, compared to our previous study (Tang et al., 2024), where the 0.7 – 55 nm fraction was assumed to contain dominantly OM complexes bridged by divalent Ca and Mg cations, along with the presence of Fe and Al oxides, the relatively high abundances of Si and Al observed here (Fig. 2a) implied the potential occurrence of clay minerals in the 0.7 – 55 nm fraction. The dominance of Al, Si, and Fe, in the 55 – 270 and 270 – 450 nm size fractions indicated the prevalence of inorganic constituents like clay minerals and Fe oxides. They can interact with the OC in these size fractions resulting in OM-mineral and/or OM-Fe oxide associations as reported in Tang et al. (2024).

4.2. *Aggregation of small SMA fractions in the presence of Fe oxides and humic acid*

Changes in the size distribution within the small SMA fraction < 20 μm occurred after the addition of Fe oxides (Fig. 1). Interactions between the added Fe oxides and particles in small SMA fractions led to the formation of the 3 – 10 μm small SMA at the expense of < 3 and > 10 μm particles (Fig. 1). Considering that the net surface charges of the added

Fe oxides (Fig. S2) and natural occurring mineral and organic particles at the lower size edge of the small SMA fractions (i.e., <1 μm colloids) were opposite under the current experimental conditions, strong electrostatic attraction occurred between the < 3 μm particles and Fe oxides resulting in their heteroaggregation. Negatively charged surfaces could derive from basal planes of clay minerals where permanent negatively charged sites exist, moreover from OM compounds, and from mineral-associated OM. The attachment of goethite or ferrihydrite on the basal sites of clay minerals was evident in SEM images (i.e., Fig. 3b and f). Moreover, SEM images revealed that the added Fe oxides could bridge colloidal- and clay-sized particles to the surface of larger size small SMA and/or primary particles (i.e., quartz; Fig. 3e). Our observations here are in line with previous studies on the interactions of Fe oxides with clay minerals, primary particles, and OM-coated particles via electrostatic attraction in model systems (i.e., Ferreiro et al., 1995; Tombácz et al., 2004; Dultz et al., 2019; Guhra et al., 2019), revealing that Fe oxides contribute to the soil aggregation at the lower hierarchical level. These interactions and aggregate formations might, in turn, help prevent Fe oxides from the abiotic/biotic dissolution (Coward et al., 2018) and thereby the release of Fe oxide associated OM.

On the other hand, the decreased abundance of > 10 μm small SMA (Table S3) implied that the added Fe oxides likely induced a rearrangement of these SMA structures. The attachment of added Fe oxides on > 10 μm small SMA and their interactions with surrounding particles might cause a contraction of aggregate structures probably via electrostatic forces. Moreover, the added Fe oxides could also enter pores of the > 10 μm small SMA, increasing contact points between particles within the > 10 μm small SMA. This likely rendered a closer packing/arrangement of particles, decreasing the abundance of the > 10 μm small SMA with a concomitant increase in the abundance of 3 − 10 μm small SMA (Table S3). Such compacting effect of Fe oxides on SMA structure has been reported for colloidal and clay-sized aggregates from the same sites (Jiang et al., 2014; Jiang et al., 2015) as well as small SMA from other arable Luvisols (Krause et al., 2020). In these studies, the removal of Fe oxides via chemical extraction resulted in an increase in sizes of < 2 μm aggregates and small SMA, presumably due to the formation of less stable structures between OM and clay minerals. In addition, the interaction between soil management and Fe oxide type (Table S2) was found to have a significant effect ($p = 0.046$) on the abundance of the > 10 μm small SMA. While their abundances were comparable ($p = 0.297$) between the goethite (13.1 ± 3.5 %) and ferrihydrite (15.4 ± 4.7 %) treatments at the bare fallow site, the abundance of the > 10 μm small SMA was notably lower ($p = 0.046$) in the ferrihydrite treatments (11.9 ± 5.4 %) than in the goethite treatments (16.9 ± 4.2 %) at the cropped site. The latter suggested a more efficient compacting effect of ferrihydrite than goethite on the SMA structure in the cropped site. This probably benefited from the small size of near-spherical ferrihydrite particles which potentially decreased the steric hindrance (Jiang et al., 2014), allowing them to enter the open pores on external surfaces of small SMA more readily than the larger goethite needles. Moreover, at the same added mass, the amount of ferrihydrite particles was likely higher than that of goethite, possibly providing more contact points between soil particles, and thereby more compact aggregate structures. Yet, variation of this effect with soil management implies that the properties of small SMA may also play a role.

Compared to the treatments with 5 wt% of Fe oxides, the less prominent changes in the size distribution by the addition of 1 wt% Fe oxides (Fig. 1; Table S2 and S3) supported the view that the mixing ratio plays a key role in the heteroaggregation of oppositely charged particles (Dultz et al., 2019; Rupp et al., 2019; Zech et al., 2020). The optimal aggregation is usually achieved at the mixing ratio when opposite surface charges were neutralized (Lagaly and Dékány, 2013), whereas excessive positive or negative surface charges often render less efficient aggregation due to prevailing repulsive forces between particles (Ritschel and Totsche, 2019; Zech et al., 2020). Moreover, by modeling the heteroaggregation of goethite and illite with different sizes, Zech et al. (2020) found that the screening effect of opposite charges is more pronounced when the size differences between the oppositely charged particles are relatively large. Instead, as the size differences between oppositely charged particles diminished, the role of geometrical constraints gets more prominent in terms of aggregation (Zech et al., 2020). In this context, the limited extent of aggregation in the 1 wt% Fe oxide addition treatments could be partially attributed to the screening effect as the amount of negatively charged particles with sizes from colloids to small SMA presumably exceeded that of the added Fe oxides.

Intriguingly, the hetero-aggregation between the added Fe oxides and particles in small SMA fractions via electrostatic interactions in suspension only fostered the formation of 3 − 10 μm small SMA. This seems to corroborate Regelink et al. (2015), who investigated the linkages among aggregate formation, porosity, and soil chemical properties of 12 soils and proposed that the contribution of Fe oxides to soil aggregation was the largest at the lowest hierarchical level. On the other hand, Rhoton et al. (2003) observed that applying ferrihydrite in an acidic silt loamy soil increased the amount of water stable macroaggregates and large SMA (53 − 250 μm) after two wet-dry cycles over 60 days. This is in line with our previous study (Tang et al., 2024), where we found that large SMA > 40 μm and macroaggregates up to 1700 μm could develop from small SMA after three successive wet-dry cycles. Also, in the current study, SEM measurements evidenced the existence of large and compact SMA up to 100 μm in the freeze-dried SMA samples from Fe oxide addition treatments (Fig. S5). These results together indicate that, besides electrostatic interaction, other physicochemical processes, like wet-dry and/or freeze–thaw cycles, may be also crucial for the contribution of Fe oxides to the aggregation at the higher hierarchical level under natural conditions.

In contrast to the Fe oxides treatments, no significant changes in the particle size distribution of SMA fractions were detected by laser diffraction in the HA treatments (Fig. 1i and j). In this study, the addition of HA was more likely to contribute to dispersion of soil particles rather than their aggregation by intensifying negative surface charges and thereby repulsive forces. The notably increased concentrations of Si, Al, and Fe in the 55 − 270 nm fraction in the HA treatments (Fig. 2b) compared to those in the controls (Fig. 2a), suggest that the HA addition might induce the release of mineral colloids from small SMA. Destabilization of aggregates and release of colloids due to the addition of HA have been reported for, i.e., the natural soil (Yan et al., 2016) and a model system of Fe oxide aggregates (Baalousha, 2009). Furthermore, the added HA tended to be adsorbed on mineral colloids rather than binding particles together, as the OC concentrations of the < 450 nm colloids notably increased upon HA addition (Fig. 2b). The carboxylic and phenolic groups in the added HA (Table S1) can support its adsorption on Fe oxides (Di Iorio et al.,2022). Moreover, the aliphatic and aromatic C compounds (Table S1) are commonly reported to be preferentially adsorbed by iron oxides (Li et al., 2023). As a result, the adsorption of HA decreased the zeta potential of colloids for both the cropped and bare fallow sites. Accordingly, the electrostatic and/or steric repulsion between particles increased, hindering their aggregation (Calero et al., 2017; Li et al., 2020). To overcome the electrostatic repulsion and to fulfill the role of OM as gluing agents, Guhra et al. (2022) proposed that external forces, i.e., supplied by compaction, gravitate sedimentation, and drying (capillary forces), are demanded. With the facilitation of external forces, distances between electrostatically repulsive particles can be reduced into the range of van der Waals interactions, thereby promoting the agglutination of particles (Guhra et al., 2022). However, it is noteworthy that the composition of OM coatings can also affect the behavior of particles. SOM comprises diverse organic compounds, such as fatty acids, lipids, amino sugars, carbohydrates, and lignin, covering great structural complexity and a wide spectrum of molecular weights/sizes. It was recently reported that adsorption of OM with a molecular weight < 3 kDa on the positively charged particles, even at a relatively high adsorbed amount, can induce aggregation of particles due to the electrostatic patch-charge attraction

(Li et al., 2020), leading to an opposite result to our observation. On the other hand, organic compounds have been proposed to be capable of forming supramolecular structures through hydrogen bonds and cation bridges (Galicia-Andrés et al., 2021; Wells and Stretz, 2019). As the molecular weight and/or size of OM increased (>3 kDa), their coatings on particles tend to promote the stabilization of particles through steric repulsion (Li et al., 2020), which is similar to our findings.

4.3. Stability of small SMA controlled by Fe oxides

During the stability test, the progressive breakdown of small SMA was reflected by the decrease in D50 and abundances of relatively large fractions (>7 μm; Fig. 4a and b; Table S4) and increased abundance of the small size fractions (i.e., <1 colloids and 1 − 7 μm particles; Fig. 4c–d; Table S4), in line with observations in previous studies on stability of aggregates using laser diffraction (Mason et al., 2011; Kasmerchak et al., 2019). For both cropped and bare fallow sites, behavior of small SMA among different treatments during the stability test was closely related to their aggregation levels, being regulated by the studied soils. Accordingly, a comparable disintegration behavior of small SMA between the 1 wt% Fe oxide addition and controls during the stability test (Fig. 4; Table S4) could be attributed to the relatively low degree of aggregation in the presence of 1 wt% Fe oxides (Fig. 1; Table S3). In these treatments, abundances of the > 10 μm small SMA, which were less involved in the aggregation process, notably decreased during the stability test (Table S4), and their breakdown into the < 7 μm small SMA was mainly responsible for the decrease in the D50 (Fig. 4; Table S4).

Conversely, in the 5 wt% Fe oxide addition treatments, the largest reduction of relative abundances of particles was found for the 7 − 10 μm SMA fraction from both the cropped and bare fallow soils (Table S4), revealing the instable nature of these small SMA formed in the presence of both goethite and ferrihydrite.Yet, the D50 in the 5 wt% goethite treatment underwent a less decline in the stability test compared to the 5 wt% ferrihydrite treatment at the cropped site, suggesting that the SMA fractions were generally better stabilized in the former treatment. Especially the > 7 μm SMA fraction, a ~ 3.5 % less disintegration of this fraction was mainly responsible for the less decrease in D50 in the 5 wt% goethite treatment at the cropped site. However, compared to the ferrihydrite treatments, more colloids were found to be released in the goethite treatments at both sites. The discrepancy in the stabilizing effect between goethite and ferrihydrite on colloids was probably caused by the difference in their sizes and shapes, which might influence their contact area with soil particles in different sizes. The contact area between particles was suggested to play a decisive role in the stability of aggregates (Dultz et al., 2019; Zech et al., 2020). The small size of ferrihydrite was likely to render a large contact area when interacting with soil colloids, supporting a tight attachment of colloids on large soil particles. For example, as shown in Fig. 3, ferrihydrite could favor the face-to-face attachment of plate-like colloids rich in clay minerals to larger particles. However, this type of attachment might be weakened in the goethite addition treatments due to the relatively large size and needle shape of goethite which likely lead to a small contact area with soil colloids. Consequently, colloidal particles in these treatments were prone to be released in the stability test. Principally, differences in the surface charge between the two added Fe oxides could also influence their interaction/aggregation with particles within SMA and thereby the stability of the resulting aggregates. The reported point of zero charge ranges from 7.9 − 8.7 and 8.0 − 8.5 for ferrihydrite and goethite (Antelo et al., 2015; Kosmulski, 2020; Mendez and Hiemstra, 2020), respectively. Accordingly, at the experimental pH (6.8 − 7.2), both the ferrihydrite and goethite are expected to be positively charged. This was confirmed by the zeta potential measurement (Fig. S2). Although the zeta potential of ferrihydrite was likely to be lower than goethite at the same pH, this difference appeared to be minor. Therefore, compared to the size and shape differences of the added Fe oxides, surface charge seemed to be less responsible for their divergent stabilizing effect on soil colloids.

Compared to the cropped site (Fig. 4e), a release of colloids was observed in the first 10 min of the stability test for the bare fallow site (Fig. 4f) in both the 5 wt% goethite and ferrihydrite addition treatments. Also, for the bare fallow site, more > 7 μm small SMA disintegrated during the stability test in the 5 wt% Fe oxide addition treatments (Table S4), leading to the largest decrease of D50 among treatments (Fig. 4b). These results suggest that the stabilizing effects of Fe oxides were less effective at the bare fallow site than the cropped one, which is contrary to our hypothesis. This was presumbly explained by the differences in small SMA properties between the soils due to the contrast management. As mentioned previously, small SMA from the cropped site contained more OC than the bare fallow site. The OC content in aggregates/soils has been frequently linked to the water stability of aggregates (e.g., Amézketa, 1999; Chenu et al., 2000). By using the laser diffraction, Kasmerchak et al., (2019) studied the behavior and stability of aggregates (without size fractionation) in different horizons of Mollisols and Alfisols. These authors observed a rapid disintegration of aggregates and release of fine particles in E horizons of these soils, where the OC contents were poor, whereas aggregates from the A horizons with the high OC content exhibited a slow disintegration particularly in Mollisols. Moreover, a relatively high OC content in the small SMA could favor the complex formation between added Fe oxides and OC, which potentially reinforced the aggregates, slowing the breakdown of SMA and release of colloids for the cropped site.

Meanwhile, it is well-known that OC/OM can interfere with the growth and transformation of poorly crystalline Fe oxides like ferrihydrite (Eusterhues et al., 2008; ThomasArrigo et al., 2019). Indeed, while the fine soil < 2 mm and occluded small SMA were more enriched in the poorly crystalline Fe oxides, their counterparts from the bare fallow soil was reported to contain relatively high amounts of total Fe oxides and crystalline Fe oxides (Siebers et al., 2024). Their coating on the particles in the small SMA fraction of the bare fallow site might increase the electrostatic repulsion between the soil particles and the added Fe oxides, which could be a possible explanation for the less stable aggregate structure. Note, the transformation of the added ferrihydrite to crystalline Fe oxides might also occur during the course of our aggregation experiment, especially in the 5 wt% ferrihydrite addition treatment for the bare fallow site, where the content of crystalline Fe oxides like goethite was relatively high. Coexistence of goethite with ferrihydrite has been evidenced to promote the formation of goethite in catalysis transformation (Notini et al., 2022). Yet, the amount of aqueous Fe(II) in our system was assumed to be low, mainly deriving from the Fe oxide suspensions. Therefore, this transformation was likely to be limited in the aggregation experiment.

In addition, the amount and type of clay minerals might be other factors that can affect the stability of aggregates (Chenu et al., 2000; Fernández-Ugalde et al., 2013). It was reported for the studied Ap horizons that the clay content in the fine soil < 2 mm at the bare fallow site was ~ 2 % higher than that at the cropped site, characterized with a high abundance of illite along with the presence of kaolinite, vermiculite, and smectite (Tang et al., 2024). Here, it is possible that the small SMA fraction in the bare fallow soil also contained more clay minerals. Moreover, the shear of smectite with swelling properties in the wet state could be relatively high in small SMA compared to the larger size aggregates, as observed in another Luvisoil (Fernández-Ugalde et al., 2013). Due to their large specific surface area, they are more active in the attachment of OC (Fernández-Ugalde et al., 2013). Under the condition of our aggregation experiment with slightly acidic pH, the Fe oxides were positively charged, and the basal and edge sites of clay minerals were likely to be negatively charged. With less presence of OC, the added Fe oxides and clay minerals in small SMA from bare fallow site could interact with each other at face as well as edge sites, resulting in voluminous structures with low contact area between particles and hence being less stable (Zech et al., 2020). Conversely, due to a relatively high OC content in the small SMA, the interaction between the

added Fe oxide and clay minerals in small SMA from the cropped site was more likely to be mediated by OC, increasing the cohesion of the formed structure. Overall, the stability of aggregates resulting from the aggregation experiment in this study was presumably dependent on the properties of the added Fe oxides (size and shape) and small SMA fractions (contents and quality of organic matter, clay fraction, and Fe oxides).

5. Conclusions

As one of the most common inorganic binding agents, Fe oxides have been reported to participate in soil aggregation at different levels. Under the studied conditions, our findings suggest that the added Fe oxides mainly contributed to the soil microaggregation in two potential ways; 1) their heteroaggregation with the < 3 μm particles in the small SMA fraction (<20 μm) presumably via electrostatic interactions, which led to the formation of the $3 - 10$ μm small SMA; and 2) rearrangement of $>$ 10 μm small SMA, rendering a more compact aggregate structure, and thereby also increasing the abundance of the $3 - 10$ μm small SMA. The latter was possibly achieved by Fe oxides entering open connective pores of the $>$ 10 μm small SMA, which could increase contact points between particles within the $>$ 10 μm small SMA. Compared to goethite needles, this compacting effect appeared to be more efficient for near-spherical ferrihydrite particles especially for the cropped site, probably due to the smaller diameter and larger specific surface area, decreasing the steric hindrance. These effects on soil microaggregation were more pronounced upon the 5 wt% Fe oxide addition, as limited aggregation likely occurred in the 1 wt% Fe oxide addition. For the latter, the positively charged surfaces of Fe oxides might be screened by the negatively charged soil compounds. Regarding the stability of aggregates formed in the presence of different Fe oxides, the size and shape differences between ferrihydrite and goethite might affect their contact areas with soil particles and thus their stabilizing effects on the formed aggregates. In addition, the stabilizing effects of Fe oxides appeared to be influenced by the properties of small SMA fractions and/or soil samples from the studied site, such as the quantity of OC and the mineralogy of Fe oxides, which can be affected by soil management.

CRediT authorship contribution statement

Ni Tang: Writing – review & editing, Writing – original draft, Visualization, Validation, Methodology, Investigation, Formal analysis, Conceptualization. **Nina Siebers:** Writing – review & editing, Validation, Resources, Project administration, Investigation, Funding acquisition, Conceptualization. **Stefan Dultz:** Writing – review & editing, Validation, Resources. **Erwin Klumpp:** Writing – review & editing, Validation, Supervision, Resources, Project administration, Funding acquisition, Conceptualization.

Declaration of competing interest

The authors declare that they have no known competing financial interests or personal relationships that could have appeared to influence the work reported in this paper.

Acknowledgements

This work is associated with the MAD Soil project (MAD Soil - Microaggregates: Formation and turnover of the structural building blocks of soils), which is funded by the DFG (Deutsche Forschungsgemeinschaft, Research Unit 2179). Ni Tang appreciates the China Scholarship Council (No. 201806190224) for supporting her studies at Forschungszentrum Jülich and RWTH Aachen University.

Appendix A. Supplementary data

Supplementary data to this article can be found online at https://doi.org/10.1016/j.geoderma.2025.117351.

Data availability

All relevant data are included in the Supplementary materials

References

Amelung, W., Tang, N., Siebers, N., Aehnelt, M., Eusterhues, K., Felde, V.J.M.N.L., Guggenberger, G., Kaiser, K., Kögel-Knabner, I., Klumpp, E., Knief, C., Kruse, J., Lehndorff, E., Mikutta, R., Peth, S., Ray, N., Prechtel, A., Ritschel, T., Schweizer, S. A., Woche, S.K., Wu, B., Totsche, K.U., 2024. Architecture of soil microaggregates: Advanced methodologies to explore properties and functions. J. Plant Nutr. Soil Sci. 187 (1), 17–50. https://doi.org/10.1002/jpln.202300149.

Amézketa, E., 1999. Soil Aggregate Stability: A Review. J. Sustain. Agric. 14 (2–3), 83–151. https://doi.org/10.1300/J064v14n02_08.

Antelo, J., Arce, F., Fiol, S., 2015. Arsenate and phosphate adsorption on ferrihydrite nanoparticles. Synergetic interaction with calcium ions. Chem. Geol. 410, 53–62. https://doi.org/10.1016/j.chemgeo.2015.06.011.

Atkinson, R.J., Posner, A.M., Quirk, J.P., 1968. Crystal nucleation in Fe(III) solutions and hydroxide gels. J. Inorg. Nucl. Chem. 30 (9), 2371–2381.

Baalousha, M., 2009. Aggregation and disaggregation of iron oxide nanoparticles: Influence of particle concentration, pH and natural organic matter. Sci. Total Environ. 407 (6), 2093–2101. https://doi.org/10.1016/j.scitotenv.2008.11.022.

Barberis, E., Marsan, F.A., Boero, V., Arduino, E., 1991. Aggregation of soil particles by iron oxides in various size fractions of soil B horizons. J. Soil Sci. 42 (4), 535–542. https://doi.org/10.1111/j.1365-2389.1991.tb00100.x.

Bieganowski, A., Ryżak, M., Sochan, A., Barna, G., Hernádi, H., Beczek, M., Polakowski, C., Makó, A., 2018. Chapter Five - Laser Diffractometry in the Measurements of Soil and Sediment Particle Size Distribution. In: Sparks, D.L. (Ed.), Advances in Agronomy. Academic Press, pp. 215–279.

Blanco-Canqui, H., Lal, R., 2004. Mechanisms of Carbon Sequestration in Soil Aggregates. Crit. Rev. Plant Sci. 23 (6), 481–504. https://doi.org/10.1080/07352680490886842.

Calero, J., Ontiveros-Ortega, A., Aranda, V., Plaza, I., 2017. Humic acid adsorption and its role in colloidal-scale aggregation determined with the zeta potential, surface free energy and the extended-DLVO theory. Eur. J. Soil Sci. 68 (4), 491–503. https://doi.org/10.1111/ejss.12431.

Chenu, C., Le Bissonnais, Y., Arrouays, D., 2000. Organic Matter Influence on Clay Wettability and Soil Aggregate Stability. Soil Sci. Soc. Am. J. 64 (4), 1479–1486. https://doi.org/10.2136/sssaj2000.6441479x.

Cornell, R.M., Schwertmann, U., 2003. The iron oxides: structure, properties, reactions, occurrences, and uses. Wiley-vch Weinheim, p. 664.

Coward, E.K., Thompson, A., Plante, A.F., 2018. Contrasting Fe speciation in two humid forest soils: insight into organomineral associations in redox-active environments. Geochim. Cosmochim. Acta 238, 68–84. https://doi.org/10.1016/j.

De-Campos, A.B., Mamedov, A.I., Huang, C.-H., 2009. Short-Term Reducing Conditions Decrease Soil Aggregation. Soil Sci. Soc. Am. J. 73 (2), 550–559. https://doi.org/10.2136/sssaj2007.0425.

Dexter, A.R., 1988. Advances in characterization of soil structure. Soil Tillage Res. 11 (3), 199–238. https://doi.org/10.1016/0167-1987(88)90002-5.

Díaz-Zorita, M., Perfect, E., Grove, J.H., 2002. Disruptive methods for assessing soil structure. Soil Tillage Res. 64 (1), 3–22. https://doi.org/10.1016/S0167-1987(01)00254-9.

Di Iorio, E., Circelli, L., Angelico, R., Torrent, J., Tan, W., Colombo, C., 2022. Environmental implications of interaction between humic substances and iron oxide nanoparticles: A review. Chemosphere 303, 135172.

Duiker, S.W., Rhoton, F.E., Torrent, J., Smeck, N.E., Lal, R., 2003. Iron (Hydr)Oxide Crystallinity Effects on Soil Aggregation. Soil Sci. Soc. Am. J. 67 (2), 606–611. https://doi.org/10.2136/sssaj2003.6060.

Dultz, S., Woche, S.K., Mikutta, R., Schrapel, M., Guggenberger, G., 2019. Size and charge constraints in microaggregation: Model experiments with mineral particle size fractions. Appl. Clay Sci. 170, 29–40. https://doi.org/10.1016/j.clay.2019.01.002.

Eusterhues, K., Wagner, F.E., Häusler, W., Hanzlik, M., Knicker, H., Totsche, K.U., Kögel-Knabner, I., Schwertmann, U., 2008. Characterization of Ferrihydrite-Soil Organic Matter Coprecipitates by X-ray Diffraction and Mössbauer Spectroscopy. Environ. Sci. Tech. 42 (21), 7891–7897.

Felde, V.J.M.N.L., Schweizer, S.A., Biesgen, D., Ulbrich, A., Uteau, D., Knief, C., Graf-Rosenfellner, M., Kögel-Knabner, I., Peth, S., 2021. Wet sieving versus dry crushing: Soil microaggregates reveal different physical structure, bacterial diversity and organic matter composition in a clay gradient. Eur. J. Soil Sci. 72 (2), 810–828. https://doi.org/10.1111/ejss.13014.

Fernández-Ugalde, O., Barré, P., Hubert, F., Virto, I., Girardin, C., Ferrage, E., Caner, L., Chenu, C., 2013. Clay mineralogy differs qualitatively in aggregate-size classes: clay-mineral-based evidence for aggregate hierarchy in temperate soils. Eur. J. Soil Sci. 64 (4), 410–422. https://doi.org/10.1111/ejss.12046.

Ferreiro, E.A., Helmy, A.K., De Bussetti, S.G., 1995. Interaction of Fe-oxyhydroxide colloidal particles with montmorillonite. Clay Miner. 30 (3), 195–200. https://doi.org/10.1180/claymin.1995.030.3.03.

Garland, G., Koestel, J., Johannes, A., Heller, O., Doetterl, S., Or, D., Keller, T., 2024. Perspectives on the misconception of levitating soil aggregates. SOIL 10 (1), 23–31. https://doi.org/10.5194/soil-10-23-2024.
Galicia-Andrés, E., Escalona, Y., Oostenbrink, C., Tunega, D., Gerzabek, M.H., 2021. Soil organic matter stabilization at molecular scale: The role of metal cations and hydrogen bonds. Geoderma 401, 115237. https://doi.org/10.1016/j.geoderma.2021.115237.
Giannetta, B., Oliveira de Souza, D., Aquilanti, G., Celi, L., Said-Pullicino, D., 2022. Redox-driven changes in organic C stabilization and Fe mineral transformations in temperate hydromorphic soils. Geoderma 406, 115532. https://doi.org/10.1016/j.geoderma.2021.115532.
Guhra, T., Ritschel, T., Totsche, K.U., 2019. Formation of mineral–mineral and organo–mineral composite building units from microaggregate-forming materials including microbially produced extracellular polymeric substances. Eur. J. Soil Sci. 70 (3), 604–615. https://doi.org/10.1111/ejss.12774.
Guhra, T., Stolze, K., Totsche, K.U., 2022. Pathways of biogenically excreted organic matter into soil aggregates. Soil Biol. Biochem. 164, 108483. https://doi.org/10.1016/j.soilbio.2021.108483.
Gui, X., Song, B., Chen, M., Xu, X., Ren, Z., Li, X., Cao, X., 2021. Soil colloids affect the aggregation and stability of biochar colloids. Sci. Total Environ. 771, 145414. https://doi.org/10.1016/j.scitotenv.2021.145414.
Gypser, S., Hirsch, F., Schleicher, A.M., Freese, D., 2018. Impact of crystalline and amorphous iron- and aluminum hydroxides on mechanisms of phosphate adsorption and desorption. J. Environ. Sci. 70, 175–189. https://doi.org/10.1016/j.jes.2017.12.001.
Henderson, R., Kabengi, N., Mantripragada, N., Cabrera, M., Hassan, S., Thompson, A., 2012. Anoxia-Induced Release of Colloid- and Nanoparticle-Bound Phosphorus in Grassland Soils. Environ. Sci. Technol. 46 (21), 11727–11734. https://doi.org/10.1021/es302395r.
Hu, W., Cichota, R., Beare, M., Müller, K., Drewry, J., Eger, A., 2023. Soil structural vulnerability: Critical review and conceptual development. Geoderma 430, 116346. https://doi.org/10.1016/j.geoderma.2023.116346.
IUSS Working Group, W., 2006. World reference base for soil resources. World Soil Resources Report 103. FAO, Rome.
Jiang, C., Séquaris, J.-M., Wacha, A., Bóta, A., Vereecken, H., Klumpp, E., 2014. Effect of metal oxide on surface area and pore size of water-dispersible colloids from three German silt loam topsoils. Geoderma 235–236, 260–270. https://doi.org/10.1016/j.geoderma.2014.07.017.
Jiang, X., Bol, R., Nischwitz, V., Siebers, N., Willbold, S., Vereecken, H., Amelung, W., Klumpp, E., 2015. Phosphorus Containing Water Dispersible Nanoparticles in Arable Soil. J. Environ. Qual. 44 (6), 1772–1781. https://doi.org/10.2134/jeq2015.02.0085.
Kaiser, M., Asefaw Berhe, A., 2014. How does sonication affect the mineral and organic constituents of soil aggregates?—A review. J. Plant Nutr. Soil Sci. 177 (4), 479–495. https://doi.org/10.1002/jpln.201300339.
Kasmerchak, C.S., Mason, J.A., Liang, M., 2019. Laser diffraction analysis of aggregate stability and disintegration in forest and grassland soils of northern Minnesota, USA. Geoderma 338, 430–444. https://doi.org/10.1016/j.geoderma.2018.06.020.
Kleber, M., Eusterhues, K., Keiluweit, M., Mikutta, C., Mikutta, R., Nico, P.S., 2015. Chapter One - Mineral–Organic Associations: Formation, Properties, and Relevance in Soil Environments. In: Sparks, D.L. (Ed.), Advances in Agronomy. Academic Press, pp. 1–140. https://doi.org/10.1016/bs.agron.2014.10.005.
Kosmulski, M., 2020. The pH dependent surface charging and points of zero charge. VIII. Update. Adv. Colloid Interface Sci. 275, 102064. https://doi.org/10.1016/j.cis.2019.102064.
Krause, L., Klumpp, E., Nofz, I., Missong, A., Amelung, W., Siebers, N., 2020. Colloidal iron and organic carbon control soil aggregate formation and stability in arable Luvisols. Geoderma 374, 114421. https://doi.org/10.1016/j.geoderma.2020.114421.
Krause, L., Rodionov, A., Schweizer, S.A., Siebers, N., Lehndorff, E., Klumpp, E., Amelung, W., 2018. Microaggregate stability and storage of organic carbon is affected by clay content in arable Luvisols. Soil and Tillage Res. 182, 123–129.
Lagaly, G., Dékány, I., 2013. Chapter 8 - Colloid Clay Science. In: Bergaya, F., Lagaly, G. (Eds.), Developments in Clay Science. Elsevier, pp. 243–345.
Lehmann, J., Kinyangi, J., Solomon, D., 2007. Organic matter stabilization in soil microaggregates: implications from spatial heterogeneity of organic carbon contents and carbon forms. Biogeochemistry 85 (1), 45–57. https://doi.org/10.1007/s10533-007-9105-3.
Li, Q., Hu, W., Li, L., Li, Y., 2023. Interactions between organic matter and Fe oxides at soil micro-interfaces: Quantification, associations, and influencing factors. Sci. Total Environ. 855, 158710. https://doi.org/10.1016/j.scitotenv.2022.158710.
Li, Z., Shakiba, S., Deng, N., Chen, J., Louie, S.M., Hu, Y., 2020. Natural Organic Matter (NOM) Imparts Molecular-Weight-Dependent Steric Stabilization or Electrostatic Destabilization to Ferrihydrite Nanoparticles. Environ. Sci. Tech. 54 (11), 6761–6770. https://doi.org/10.1021/acs.est.0c01189.
Mason, J.A., Greene, R.S.B., Joeckel, R.M., 2011. Laser diffraction analysis of the disintegration of aeolian sedimentary aggregates in water. Catena 87 (1), 107–118. https://doi.org/10.1016/j.catena.2011.05.015.
Mendez, J.C., Hiemstra, T., 2020. Surface area of ferrihydrite consistently related to primary surface charge, ion pair formation, and specific ion adsorption. Chem. Geol. 532, 119304. https://doi.org/10.1016/j.chemgeo.2019.119304.
Meyer, N., Bornemann, L., Welp, G., Schiedung, H., Herbst, M., Amelung, W., 2017. Carbon saturation drives spatial patterns of soil organic matter losses under long-term bare fallow. Geoderma 306, 89–98. https://doi.org/10.1016/j.geoderma.2017.07.004.
Mitchell, J.K., Soga, K., 2005. Fundamentals of soil behavior, 3. John Wiley & Sons New York.
Oades, J., Waters, A., 1991. Aggregate hierarchy in soils. Soil Res. 29 (6), 815–828. https://doi.org/10.1071/SR9910815.
Notini, L., ThomasArrigo, L.K., Kaegi, R., Kretzschmar, R., 2022. Coexisting Goethite Promotes Fe(II)-Catalyzed Transformation of Ferrihydrite to Goethite. Environ. Sci. Tech. 56 (17), 12723–12733. https://doi.org/10.1021/acs.est.2c03925.
Peng, X., Yan, X., Zhou, H., Zhang, Y.Z., Sun, H., 2015. Assessing the contributions of sesquioxides and soil organic matter to aggregation in an Ultisol under long-term fertilization. Soil Tillage Res. 146, 89–98. https://doi.org/10.1016/j.still.2014.04.003.
Pinheiro-Dick, D., Schwertmann, U., 1996. Microaggregates from Oxisols and Inceptisols: dispersion through selective dissolutions and physicochemical treatments. Geoderma 74 (1), 49–63. https://doi.org/10.1016/S0016-7061(96)00047-X.
Regelink, I.C., Stoof, C.R., Rousseva, S., Weng, L., Lair, G.J., Kram, P., Nikolaidis, N.P., Kercheva, M., Banwart, S., Comans, R.N.J., 2015. Linkages between aggregate formation, porosity and soil chemical properties. Geoderma 247–248, 24–37. https://doi.org/10.1016/j.geoderma.2015.01.022.
Rhoton, F.E., Römkens, M.J.M., Bigham, J.M., Zobeck, T.M., Upchurch, D.R., 2003. Ferrihydrite Influence on Infiltration, Runoff, and Soil Loss. Soil Sci. Soc. Am. J. 67 (4), 1220–1226. https://doi.org/10.2136/sssaj2003.1220.
Ritschel, T., Totsche, K.U., 2019. Modeling the formation of soil microaggregates. Comput. Geosci. 127, 36–43. https://doi.org/10.1016/j.cageo.2019.02.010.
Rupp, A., Guhra, T., Meier, A., Prechtel, A., Ritschel, T., Ray, N., Totsche, K.U., 2019. Application of a Cellular Automaton Method to Model the Structure Formation in Soils Under Saturated Conditions: A Mechanistic Approach. Front. Environ. Sci. 7. https://doi.org/10.3389/fenvs.2019.00170.
Schweizer, S.A., Aehnelt, M., Bucka, F., Totsche, K.U., Kögel-Knabner, I., 2024. Impact of bare fallow management on soil carbon storage and aggregates across a rock fragment gradient. J. Plant Nutr. Soil Sci. 187 (1), 118–129. https://doi.org/10.1002/jpln.202300156.
Schweizer, S.A., Bucka, F.B., Graf-Rosenfellner, M., Kögel-Knabner, I., 2019. Soil microaggregate size composition and organic matter distribution as affected by clay content. Geoderma 355, 113901. https://doi.org/10.1016/j.geoderma.2019.113901.
Schwertmann, U., Taylor, R.M., 1989. Iron Oxides, Minerals in Soil Environments. SSSA Book Series, pp. 379-438. https://doi.org/10.2136/sssabookser1.2ed.c8.
Schwertmann, U., Cornell, R.M., 2008. Iron oxides in the laboratory: preparation and characterization. John Wiley & Sons.
Siebers, N., Abdelrahman, H., Krause, L., Amelung, W., 2018. Bias in aggregate geometry and properties after disintegration and drying procedures. Geoderma 313, 163–171. https://doi.org/10.1016/j.geoderma.2017.10.028.
Siebers, N., Voggenreiter, E., Joshi, P., Rethemeyer, J., Wang, L., 2024. Synergistic relationships between the age of soil organic matter, Fe speciation, and aggregate stability in an arable Luvisol. J. Plant Nutr. Soil Sci. 187 (1), 77–88. https://doi.org/10.1002/jpln.202300020.
Six, J., Bossuyt, H., Degryze, S., Denef, K., 2004. A history of research on the link between (micro)aggregates, soil biota, and soil organic matter dynamics. Soil Tillage Res. 79 (1), 7–31. https://doi.org/10.1016/j.still.2004.03.008.
Tang, N., Dultz, S., Gerth, D., Klumpp, E., 2024. Soil colloids as binding agents in the formation of soil microaggregates in wet-dry cycles: A case study for arable Luvisols under different management. Geoderma 443, 116830. https://doi.org/10.1016/j.geoderma.2024.116830.
ThomasArrigo, L.K., Kaegi, R., Kretzschmar, R., 2019. Ferrihydrite Growth and Transformation in the Presence of Ferrous Iron and Model Organic Ligands. Environ. Sci. Tech. 53 (23), 13636–13647. https://doi.org/10.1021/acs.est.9b03952.
Tombácz, E., Libor, Z., Illés, E., Majzik, A., Klumpp, E., 2004. The role of reactive surface sites and complexation by humic acids in the interaction of clay mineral and iron oxide particles. Org. Geochem. 35 (3), 257–267. https://doi.org/10.1016/j.orggeochem.2003.11.002.
Totsche, K.U., Amelung, W., Gerzabek, M.H., Guggenberger, G., Klumpp, E., Knief, C., Lehndorff, E., Mikutta, R., Peth, S., Prechtel, A., Ray, N., Kögel-Knabner, I., 2018. Microaggregates in soils. J. Plant Nutr. Soil Sci. 181 (1), 104–136. https://doi.org/10.1002/jpln.201600451.
Virto, I., Barré, P., Chenu, C., 2008. Microaggregation and organic matter storage at the silt-size scale. Geoderma 146 (1), 326–335. https://doi.org/10.1016/j.geoderma.2008.05.021.
Wagai, R., Kajiura, M., Uchida, M., Asano, M., 2018. Distinctive Roles of Two Aggregate Binding Agents in Allophanic Andisols: Young Carbon and Poorly-Crystalline Metal Phases with Old Carbon. Soil Syst. 2 (2), 29. https://www.mdpi.com/2571-8789/2/2/29.
Wells, M.J.M., Stretz, H.A., 2019. Supramolecular architectures of natural organic matter. Science of the Total Environment 671, 1125–1133. https://doi.org/10.1016/j.scitotenv.2019.03.406.
Yan, J., Lazouskaya, V., Jin, Y., 2016. Soil Colloid Release Affected by Dissolved Organic Matter and Redox Conditions. Vadose Zone J. 15 (3). https://doi.org/10.2136/vzj2015.02.0026.
Yang, W., Shang, J., Sharma, P., Li, B., Liu, K., Flury, M., 2019. Colloidal stability and aggregation kinetics of biochar colloids: Effects of pyrolysis temperature, cation

type, and humic acid concentrations. Sci. Total Environ. 658, 1306–1315. https://doi.org/10.1016/j.scitotenv.2018.12.269.
Xue, B., Huang, L., Huang, Y., Zhou, F., Li, F., Kubar, K.A., Li, X., Lu, J., Zhu, J., 2019. Roles of soil organic carbon and iron oxides on aggregate formation and stability in two paddy soils. Soil Tillage Res. 187, 161–171. https://doi.org/10.1016/j.still.2018.12.010.
Zech, S., Dultz, S., Guggenberger, G., Prechtel, A., Ray, N., 2020. Microaggregation of goethite and illite evaluated by mechanistic modeling. Appl. Clay Sci. 105845. https://doi.org/10.1016/j.clay.2020.105845.